



Universiteit
Leiden
The Netherlands

Immune modulation by schistosomes : mechanisms of T helper 2 polarization and implications for metabolic disorders

Hussaarts, L.

Citation

Hussaarts, L. (2015, September 10). *Immune modulation by schistosomes : mechanisms of T helper 2 polarization and implications for metabolic disorders*. Retrieved from <https://hdl.handle.net/1887/35155>

Version: Not Applicable (or Unknown)

License: [Leiden University Non-exclusive license](#)

Downloaded from: <https://hdl.handle.net/1887/35155>

Note: To cite this publication please use the final published version (if applicable).

Cover Page



Universiteit Leiden

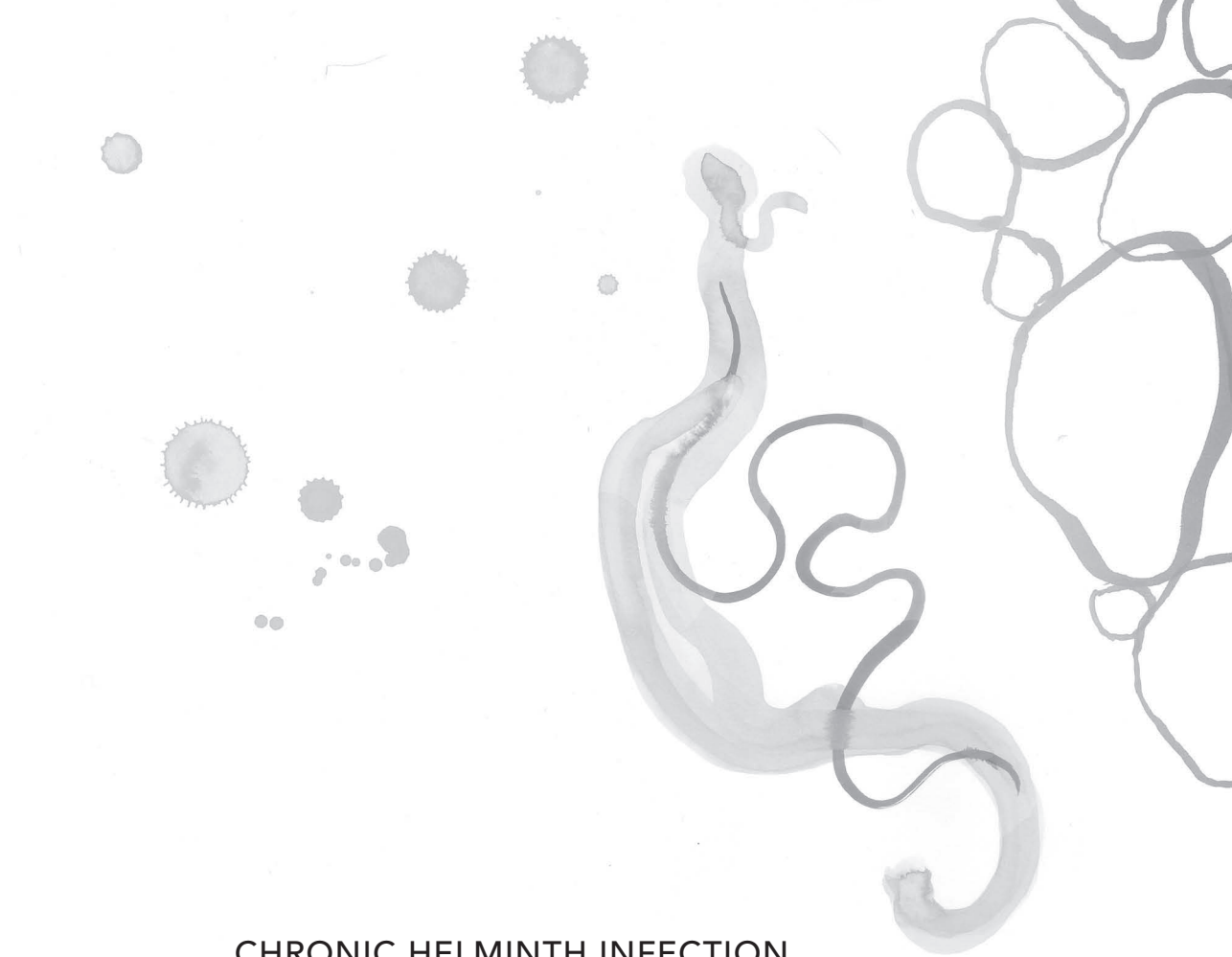


The handle <http://hdl.handle.net/1887/35155> holds various files of this Leiden University dissertation.

Author: Hussaarts, Leonie

Title: Immune modulation by schistosomes : mechanisms of T helper 2 polarization and implications for metabolic disorders

Issue Date: 2015-09-10



CHRONIC HELMINTH INFECTION
AND HELMINTH-DERIVED EGG
ANTIGENS PROMOTE ADIPOSE
TISSUE M2 MACROPHAGES AND
IMPROVE INSULIN SENSITIVITY
IN OBESE MICE

Leonie Hussaarts, Noemí García-Tardón,
Lianne van Beek, Mattijs M. Heemskerk, Simone Haeberlein,
Gerard C. van der Zon, Arifa Ozir-Fazalalikhan,
Jimmy F. P. Berbée, Ko Willems van Dijk,
Vanessa van Harmelen, Maria Yazdanbakhsh
and Bruno Guigas

*The FASEB Journal, published online ahead of print
in April 2015. doi:10.1096/fj.14-262329*

5

ABSTRACT

Chronic low-grade inflammation associated with obesity contributes to insulin resistance and type 2 diabetes. Helminth parasites are the strongest natural inducers of type 2 immune responses, and short-lived infection with rodent nematodes was reported to improve glucose tolerance in obese mice. Here, we investigated the effects of chronic infection (12 weeks) with *Schistosoma mansoni*, a helminth that infects millions of humans worldwide, on whole-body metabolic homeostasis and white adipose tissue (WAT) immune cell composition in high-fat diet-induced obese C57BL/6 male mice. Our data indicate that chronic helminth infection reduced body weight gain (-62%), fat mass gain (-89%) and adipocyte size; lowered whole-body insulin resistance (-23%) and glucose intolerance (-16%); and improved peripheral glucose uptake (+25%) and WAT insulin sensitivity. Analysis of immune cell composition by flow cytometry and quantitative PCR revealed that *S. mansoni* promoted strong increases in WAT eosinophils and alternatively activated M2 macrophages. Importantly, injections with *S. mansoni* soluble egg antigens recapitulated the beneficial effect of parasite infection on whole-body metabolic homeostasis and induced type 2 immune responses in WAT and liver. Taken together, we provide novel data suggesting that chronic helminth infection and helminth-derived molecules protect against metabolic disorders by promoting a T helper 2 response, eosinophilia and WAT M2 polarization.

INTRODUCTION

The obesity epidemic represents a growing threat to public health, not only in industrialized countries but also in urban centers of developing countries. Obesity significantly increases the risk for the development of type 2 diabetes, cardiovascular diseases, and eventually cancer (1;2) and is often associated with a state of chronic, low-grade inflammation, which contributes to tissue-specific insulin resistance and whole-body metabolic dysfunction (3). Among the underlying molecular mechanisms, classically activated (M1) macrophages were shown to accumulate in white adipose tissue (WAT) from obese mice, where they secrete pro-inflammatory cytokines such as interleukin (IL)-1 β and tumor necrosis factor- α (TNF- α) (4-6). These cytokines interfere with insulin signaling (7;8) and induce lipolysis (9;10), thereby increasing circulating free fatty acids which promote peripheral insulin resistance (11). Other immune cell types, including neutrophils (12), mast cells (13), B cells (14;15) and CD8⁺ T cells (16), have also been shown to mediate insulin resistance.

By contrast, alternatively activated (M2) macrophages prevail in lean WAT and are involved in the maintenance of adipose tissue insulin sensitivity, partly through secretion of the anti-inflammatory cytokine IL-10 (6;17). The M2 phenotype is promoted by T helper 2 (Th2)-type cytokines like IL-4, secreted by WAT eosinophils (18), and IL-5 and IL-13, released from WAT innate lymphoid type 2 cells (ILC2s) (19). In addition, Th2 and regulatory T cell responses, as well as administration of IL-4, have been associated with protection against insulin resistance (20-22). Together, these studies illustrate that type 2 and anti-inflammatory responses are beneficial for the expanding adipose tissue environment and the maintenance of tissue-specific insulin sensitivity and whole-body glucose homeostasis.

Helminth parasites are the strongest natural inducers of type 2 inflammatory responses, and epidemiological studies in India and rural China revealed that helminth infections inversely correlate with metabolic syndrome (23-25). In addition, seminal papers recently reported that the rodent nematode *Nippostrongylus brasiliensis*, which is spontaneously cleared within two weeks of infection, improves glucose tolerance in diet-induced obese mice (18;26), associated with WAT eosinophilia (18) or increased M2 gene expression (26). Furthermore, *Schistosoma mansoni* soluble egg antigens could protect against atherosclerosis in hyperlipidemic LDLR knockout mice (27). These studies suggest that manipulation of the immune system by helminths or their molecules might be beneficial for metabolic homeostasis. However, it remains unclear which aspects of whole-body energy metabolism are affected by the worms, and the immunological changes that take place in WAT have not yet been characterized at the cellular level.

Furthermore, as most helminth infections in humans are chronic in nature, it would be important to test whether the beneficial effect on metabolic homeostasis also occurs in a model of chronic infection. Of the various helminth species, schistosomes are among the most prevalent and chronically infect millions of people worldwide (28). While infection with *N. brasiliensis* induces a strong Th2 response that mediates parasite rejection within two weeks after infection, the Th2 response in schistosomiasis emerges after 5-6 weeks of infection,

with the onset of egg production that also triggers the development of M2 macrophages (29). In most individuals, infection often reaches a chronic stage, characterized by a decline in Th2 inflammation and the presence of regulatory B and T cells (30;31). In the present study, we therefore investigated the impact of *S. mansoni* infection for 12 weeks on whole-body metabolic homeostasis, WAT insulin sensitivity, and WAT immune cell composition in mice fed either low- or high-fat diet (HFD). Next, to study the impact of helminth-derived molecules on metabolic disorders in a pathogen-free setting, we treated HFD-fed mice with *S. mansoni* soluble egg antigens (SEA) for 4 weeks and assessed whole-body glucose tolerance and insulin sensitivity, and the immune cell composition of WAT and liver.

MATERIALS AND METHODS

Animals, diet and *S. mansoni* infection

All mouse experiments were performed in accordance with the Guide for the Care and Use of Laboratory Animals of the Institute for Laboratory Animal Research and have received approval from the university Ethical Review Boards (Leiden University Medical Center, Leiden, The Netherlands; DEC2189). Male C57BL/6J mice (8-10 weeks old; Charles River, L'Arbresle Cedex, France) were housed in a temperature-controlled room with a 12-hour light-dark cycle. Throughout the experiment, food and tap water were available *ad libitum*. Mice were fed a high-fat diet (45% energy derived from fat, D12451, Research Diets, Wijk bij Duurstede, The Netherlands) or a low-fat diet (10% energy derived from fat, D12450B, Research Diets), which were similar in composition in all respects apart from the total fat content. After 6 weeks, mice were randomized according to body weight and fasting plasma glucose and insulin levels and percutaneously infected with 36 *S. mansoni* cercariae, as previously described (32). Mice were monitored for 12 additional weeks. The effects of chronic infection were assessed in 2 independent experiments. Before SEA injections, mice were fed a LFD or HFD for 12 weeks after which they were randomized according to body weight, fasting plasma glucose and insulin levels, and fat mass. SEA (50 µg) was injected intraperitoneally once every 3 days for a period of 4 weeks. The effects of SEA treatment were assessed in 2 independent experiments.

Plasma analysis

Blood samples were collected from the tail tip of 4-hour-fasted mice (food removed at 9 am) by use of chilled capillaries. Blood glucose level was determined by use of a glucometer (Accu-Check, Roche Diagnostics Almere, The Netherlands) and plasma insulin level was measured by use of a commercial kit according to the instructions of the manufacturer (Millipore, The Netherlands).

Glucose and insulin tolerance tests

The effect of chronic *S. mansoni* infection on glucose tolerance was assessed by intravenous glucose tolerance test (ivGTT) at week 5 and 11 postinfection. Mice were fasted for 6 hours, and the tests were carried out at 2 pm. After an initial blood collection ($t=0$), a glucose

load (2g D-Glucose/kg total body weight of which 50% of the glucose was [6,6-²H₂]glucose (Sigma-Aldrich, Zwijndrecht, The Netherlands) was administered in conscious mice via injection in the tail vein. Blood sampling was performed by tail bleeding at 2.5, 15, 30, 60, 90 and 120 minutes: 5-10 μ L whole blood was spotted on sample carrier paper (Sartorius Stedim, Goettingen, Germany) and an additional drop was used to measure glucose using a glucometer (Accu-Check, Roche Diagnostics). To analyze peripheral glucose uptake, blood spot glucose enrichment was measured by extracting glucose from the filter paper with 75 μ L water (B. Braun, Oss, Netherlands) and 1 mL methanol. The extracted glucose was derivatized to aldonitrile penta-acetate and reconstituted in 100 μ L ethyl acetate, of which 1 μ L was injected for gas chromatography (HP6890II) mass spectrometry (HP5973, Hewlett-Packard Co., Palo Alto, CA, USA), as described previously (33). Mass-over-charge ratios of 187, 188 and 189 were monitored in selective ion monitoring mode, from which the percentage of unlabeled and labeled glucose was calculated based on theoretical isotopic distribution. Concentrations of labeled glucose were calculated based on the plasma glucose levels, and values were natural log-transformed after which a decay curve was fitted. Individual decay curves were calculated, of which the slope represents the peripheral glucose uptake. The effect of SEA treatment on glucose tolerance was assessed by an i.p. glucose tolerance test (2 g D-Glucose/kg total body weight) in 6-hour fasted mice at week 3 postinjections.

Whole-body insulin sensitivity was determined by an intraperitoneal insulin tolerance test (ITT) at 5 and 11 weeks postinfection or at week 3 post-SEA treatment. Mice were fasted for 4 hours, and the tests were carried out at 1 pm. After an initial blood collection ($t=0$), an intraperitoneal bolus of insulin (1 U/kg lean body mass; NOVORAPID, Novo Nordisk, Alphen aan den Rijn, Netherlands) was administered to the mice. Blood glucose was measured by tail bleeding at 15, 30, 60, and 120 minutes after insulin administration by use of a glucometer.

Body composition and indirect calorimetry

Body composition was measured by MRI using an EchoMRI (Echo Medical Systems, Houston, TX, USA). Groups of 8 mice with free access to food and water were subjected to individual indirect calorimetric measurements at week 11 postinfection for a period of 7 consecutive days using a Comprehensive Laboratory Animal Monitoring System (Columbus Instruments, Columbus, OH, USA). Before the start of the measurements, the animals were acclimated to the cages and the single housing for a period of 48 hours. Feeding behavior was assessed by real-time food intake. Spontaneous locomotor activity was determined by the measurement of beam breaks. Oxygen consumption and carbon dioxide production were measured at 15-minute intervals and normalized for body surface area ($\text{kg}^{0.75}$). Respiratory exchange ratio and energy expenditure were calculated as described previously (34).

Isolation of adipocytes and stromal vascular fraction (SVF) from adipose tissue

Gonadal (epididymal), visceral (mesenteric) and subcutaneous (flank) adipose tissues were collected from infected and uninfected mice, minced, and digested for 1 h at 37°C in HEPES buffer (pH 7.4) containing 0.5g/l type 1 collagenase from *Clostridium histolyticum* (Sigma-Aldrich)

and 2% (w/v) dialyzed bovine serum albumin (Fraction V; Sigma-Aldrich). The disaggregated adipose tissue was filtered through a 236 μm nylon mesh. Mature adipocytes were isolated from the surface of the filtrate and washed several times with PBS. Cell size was determined using an imaging technique implemented in MATLAB which automatically determines size of isolated adipocytes from microscopic pictures (~1000 cells/fat tissue sample). The adipocyte size distribution, mean adipocyte diameter and volume, and adipocyte number per fat pad were calculated, as described previously (35). The residue of the gonadal and visceral adipose tissue filtrate was used for the isolation of stromal vascular cells for flow cytometry. In brief, after centrifugation (350 g , 10 minutes, room temperature), the supernatant was discarded and the pellet was treated with erythrocyte lysis buffer. The cells were washed twice with PBS and counted manually or using an automated cell counter (TC10, Bio-Rad, Hercules, CA, USA). Following SEA injections, stromal vascular cells from gonadal adipose tissue were isolated as described above, with the exception that the disaggregated adipose tissue was passed through a 100 μm cell strainer that was washed with PBS supplemented with 2.5 mM EDTA and 5% fetal calf serum (FCS).

Isolation of CD45⁺ cells from liver tissue

Livers were minced and digested for 45 minutes at 37°C in RPMI 1640 + Glutamax (Life Technologies, Bleiswijk, The Netherlands) containing 1 mg/mL collagenase type IV from *Clostridium histolyticum*, 2000 U/mL DNase (both Sigma-Aldrich), and 1 mM CaCl_2 . The digested liver tissues were passed through 100 μm cell strainers that were washed with PBS supplemented with 2.5 mM EDTA and 5% FCS. Following centrifugation (530 g , 10 minutes, 4°C), the supernatant of the filtrate was discarded, after which the pellet was resuspended in PBS + 2.5 mM EDTA and 5% FCS and centrifuged at 50 g to remove hepatocytes (3 minutes, 4 degrees). Next, supernatants were collected and pelleted (530 g , 10 minutes, 4°C). The pellet was treated with erythrocyte lysis buffer, and the cells were washed once more with PBS + 2.5 mM EDTA and 5% FCS. CD45⁺ cells were isolated by use of LS columns and CD45 MicroBeads (35 μL /liver; Miltenyi Biotec, Bergisch Galdbach, Germany) according to manufacturer's protocol. Isolated CD45⁺ cells were counted and processed as described for the SVF.

Processing of isolated cells for flow cytometry

For analysis of macrophage and lymphocyte subsets, isolated stromal vascular cells and CD45⁺ cells from liver were stained with the live/dead marker Aqua (Invitrogen), after which they were fixed with 1.9% paraformaldehyde (Sigma-Aldrich) and stored in FACS buffer (PBS, 0.02% sodium azide, 0.5% FCS) at 4°C in the dark until subsequent analysis. For analysis of cytokine production, isolated cells were cultured for 4 hours in culture medium in the presence of 100 ng/mL phorbol myristate acetate (PMA), 1 $\mu\text{g}/\text{mL}$ ionomycin and 10 $\mu\text{g}/\text{mL}$ Brefeldin A (all Sigma-Aldrich). After culture, cells were washed with PBS, stained with Aqua, and fixed as described above.

Flow cytometry

For analysis of lymphocyte subsets, SVF cells were stained with antibodies against CD4 (GK1.5), CD3 (17A2), B220 (RA3-6B2) or CD19 (1D3; all eBioscience, San Diego, CA, USA), CD8 (53-6.7), CD45 (104; both BioLegend, San Diego, CA, USA) and NK1.1 (PK136, eBioscience or BD Biosciences, San Jose, CA, USA). Following SEA injections, when ILC2s were analyzed, additional antibodies were included against Thy1.2 (52-2.1), CD11b (M1/7; both eBioscience), CD11c (HL3) and GR-1 (RB6-8C5; both BD Biosciences), to gate on lineage-negative Thy1.2⁺ cells. For analysis of macrophages and eosinophils, cells were permeabilized with 0.5% saponin (Sigma-Aldrich) in which they were also stained. Cells were incubated with an antibody against Ym1 conjugated to biotin (R&D Systems, Minneapolis, MN, USA), washed, and stained with streptavidin-PerCP (BD Biosciences) and antibodies directed against CD45, CD11b, CD11c, F4/80 (BM8; eBioscience), Siglec-F (E50-2440; BD Biosciences), and following SEA injections, Ly6C (HK1.4; BioLegend). Cytokine production of Th2 cells and ILC2s was analyzed following permeabilization, as described above, using antibodies against CD11b, CD11c, GR-1, B220, NK1.1, CD3, CD45, CD4, Thy1.2, IL-4 (11B11; eBioscience), IL-13 (eBio13A; eBioscience) and IL-5 (TRFK5; BioLegend). Flow cytometry was performed using a FACSCanto (BD Biosciences), and gates were set according to Fluorescence Minus One (FMO) controls. Representative gating schemes are shown in Supplemental Fig. 1.

In vivo insulin signaling

Mice were food-deprived for 4 hours and subjected to an i.p. injection of human recombinant insulin (1 U/kg body weight; NOVORAPID, Novo Nordisk) at 1 pm. Mice were sacrificed after 15 minutes and gonadal and visceral adipose tissues were isolated and immediately snap-frozen. Subsequently, the tissue samples (~30 mg) were lysed in ice-cold buffer containing 50 mM Hepes (pH 7.6), 50 mM NaF, 50 mM KCl, 5 mM NaPPi, 1 mM EDTA, 1 mM EGTA, 1 mM DTT, 5 mM β -glycerophosphate, 1 mM sodium vanadate, 1% NP40 and protease inhibitor cocktail (Complete, Roche Diagnostics). Western blots were performed using phospho-specific (Thr308-PKB, Cell Signaling Technology, Leiden, The Netherlands) or total primary antibodies (tubulin from Cell Signalling; insulin receptor β (IR β) from Santa Cruz Biotechnology, Dallas, TX, USA), as described previously (36). Bands were visualized by enhanced chemiluminescence and quantified by use of ImageJ (NIH, Bethesda, MD, USA).

RNA purification and qRT-PCR

RNA was extracted from snap-frozen tissue samples (~20 mg) using Tripure RNA Isolation reagent (Roche Diagnostics). Total RNA (1 μ g) was reverse transcribed and quantitative real-time PCR was then performed with SYBR Green Core Kit on a MyIQ thermal cycler (Bio-Rad) using specific primers sets: 5'-GCCACCAACCCTCCTGGCTG-3' (Itgax-R), 5'-TTGGACTCTGCTGTGCAGTTG-3' (Itgax-F), 5'-GTCCCAAAGGGATGAGAAG-3' (Tnfa-R), 5'-CACTTGGTGGTTTGCTACGA-3' (Tnfa-F), 5'-TCCTGGACATTACGACCCT-3' (Nos2-R), 5'-CTCTGAGGGCTGACACAAGG-3' (Nos2-F), 5'-TCAGCCAGATGCAGTTAACGCC-3' (Ccl2-R), 5'-GCTTCTTTGGACACCTGCTGCT-3' (Ccl2-F), 5'-CCTGCCCTGCTGGGATGACT-3' (Retnla-R), 5'-GGGCAGTGGTCCAGTCAACGA-3' (Retnla-F),

5'-ACAATTAGTACTGGCCACCAGGAA-3' (Chil3-R), 5'-TCCTTGAGCCACTGAGCCTTCA-3' (Chil3-F), 5'-GACCACGGGGACCTGGCCTT-3' (Arg1-R), 5'-ACTGCCAGACTGTGGTCTCCACC-3' (Arg1-F), 5'-CCTCACAGCAACGAAGAACA-3' (Il4-R), 5'-ATCGAAAAGCCCCGAAAGAGT-3' (Il4-F), 5'-TGGGGGTACTGTGGAAATGC-3' (Il5-R), 5'-CCACACTTCTTTTTTGGCGG-3' (Il5-F), 5'-CCCTGGATTCCCTGACCAAC-3' (Il13-R), 5'-GGAGGCTGGAGACCGTAGT-3' (Il13-F), 5'-CTTTGGCTATGGGCTCCAGTC-3' (Emr1-R), 5'-GCAAGGAGGACAGAGTTTATCGTG-3' (Emr1-F), 5'-ACTGAAGTACCAAATGGACAATGTTAGT-3' (Clec4f-R), 5'-GTCAGCATTACATCCTCCAGA-3' (Clec4f-F). mRNA expression was normalized to RplP0 mRNA content and expressed as fold change compared to noninfected LFD-fed mice using the $\Delta\Delta$ CT method.

Statistical analysis

All data are presented as means \pm SEM. Statistical analysis was performed using GraphPad Prism version 6.00 for Windows (GraphPad Software, La Jolla, CA, USA) with 2-tailed unpaired Student's *t* test. Differences between groups were considered statistically significant at $P < 0.05$. For repeated measurements, data were analyzed assuming the same scatter to increase power.

RESULTS

Chronic *S. mansoni* infection reduces fat mass in HFD-induced obese mice

To study the effect of chronic helminth infection on whole-body energy homeostasis, C57BL/6 male mice were fed a LFD or HFD for 6 weeks, before infection with *S. mansoni* for 12 additional weeks. HFD induced a time-dependent increase in body weight (Fig. 1A), fat mass (Fig. 1B,C), and mean adipocyte volume (Fig. 1D) when compared with LFD-fed mice. In response to *S. mansoni* infection, HFD-fed mice gained significantly less weight (Fig. 1A), an effect exclusively resulting from a reduction in body fat mass without affecting lean body mass (Fig. 1B,C). Morphometric analysis of various WATs revealed that chronic *S. mansoni* infection reduced HFD-induced adipocyte hypertrophy (Fig. 1D), while cell numbers remained unaffected (data not shown). In LFD-fed animals, *S. mansoni* induced a small but significant decrease in gonadal adipocyte mean volume, but did not affect body weight and fat mass. Next, by use of metabolic cages, we found that food intake and spontaneous locomotor activity were not affected by chronic infection (Fig. 1E,F), and indirect calorimetry also revealed that infection did not affect the respiratory exchange ratio (Fig. 1G) or energy expenditure (Fig. 1H) in HFD-fed animals.

Chronic *S. mansoni* infection improves whole-body glucose tolerance and insulin sensitivity in HFD-induced obese mice

We next investigated the effect of chronic *S. mansoni* infection on whole-body metabolic homeostasis in lean and HFD-induced obese mice. As expected, HFD increased fasting plasma glucose and insulin levels (Fig. 2A), and HOMA-IR (HOMeostatis Model Assessment of Insulin Resistance; Fig. 2B). In addition, HFD impaired whole-body glucose tolerance (Fig. 2C,D), peripheral glucose uptake (Fig. 2E,F), and insulin sensitivity (Fig. 2G,H). Chronic *S. mansoni* infection restored fasting blood glucose and insulin levels in mice on HFD (Fig. 2A), resulting

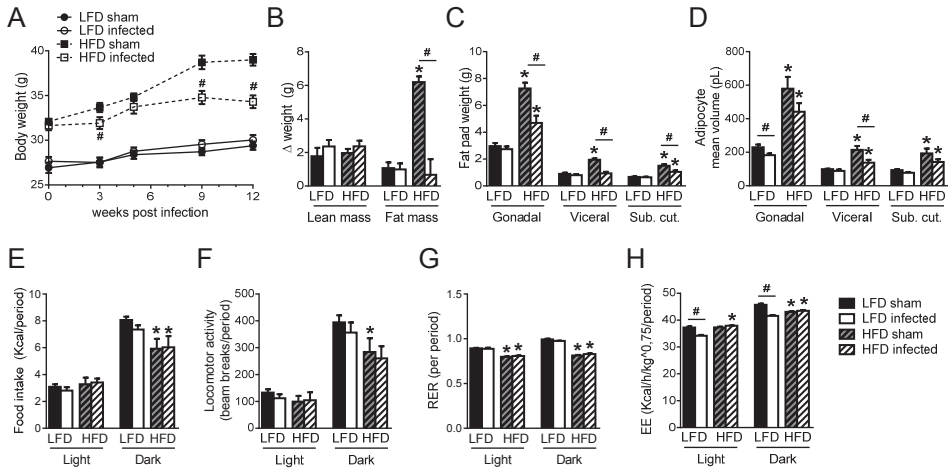


Figure 1. Chronic *S. mansoni* infection reduces body weight gain, fat mass and adipocyte size in diet-induced obese mice. Mice were fed a LFD or HFD for 6 weeks before infection with *S. mansoni* cercariae or sham-infection for 12 weeks. Body weight was monitored throughout the experimental period (A). The change in body composition from the start of infection (B), weight of different fat pads (C) and adipocyte mean volume (D) were measured at week 12 postinfection. Food intake (E), spontaneous locomotor activity (F), respiratory exchange ratio (RER; G) and energy expenditure (EE; H) were assessed using fully automated single-housed metabolic cages during week 11. Results are expressed as means \pm SEM. * $P < 0.05$ HFD vs LFD, # $P < 0.05$ helminth- vs sham-infected group ($n = 4-11$ animals per group in B, D-H, and 12-19 animals per group in A, C).

in a time-dependent reduction in HOMA-IR (Fig. 2B). Furthermore, chronic infection restored HFD-induced whole-body glucose tolerance (Fig. 2C,D), improved peripheral glucose uptake (Fig. 2E,F) and promoted whole-body insulin sensitivity (Fig. 2G,H). Of note, except for a slight but significant decrease in fasting plasma insulin level, *S. mansoni* infection did not affect any metabolic parameters in LFD-fed mice. Overall, these data indicate that *S. mansoni* improves whole-body glucose tolerance and insulin resistance in diet-induced obese mice.

Chronic *S. mansoni* infection improves adipose tissue insulin sensitivity in HFD-induced obese mice

To study the effect of chronic *S. mansoni* infection on WAT-specific insulin sensitivity, mice were subjected to an acute intraperitoneal insulin injection. The expression of IR β and insulin-induced phosphorylation of protein kinase B (PKB) were assessed by Western Blot in both gonadal and visceral WAT. As expected, HFD reduced IR β protein expression (Fig. 2I,K) and impaired PKB phosphorylation in response to insulin (Fig. 2J,K) in both gonadal and visceral WAT, indicating tissue-specific insulin resistance. Chronic *S. mansoni* infection restored IR β protein expression and insulin-induced PKB phosphorylation in WAT of HFD-fed mice (Fig. 2I-K), suggesting that the beneficial effect of helminths observed at the systemic level might be secondary to improved tissue-specific insulin sensitivity.

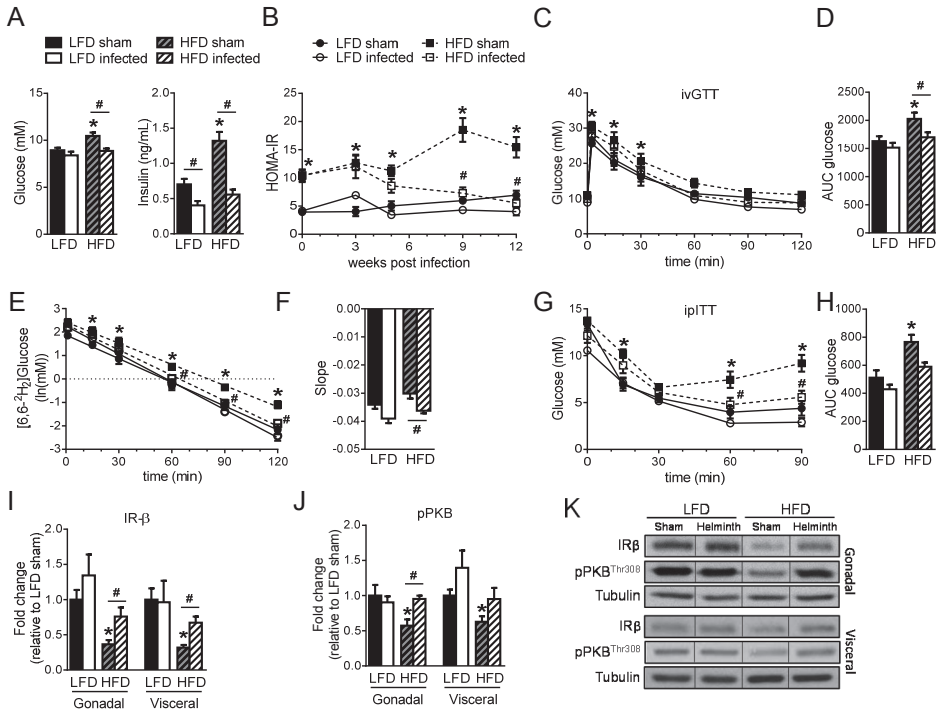


Figure 2. Chronic *S. mansoni* infection improves whole-body glucose tolerance and insulin sensitivity in diet-induced obese mice. Mice were fed a LFD or HFD and were infected with *S. mansoni* as described in the legend of Fig. 1. Plasma glucose and insulin levels (A) were determined in 4h-fasted mice at week 12 postinfection. HOMA-IR was calculated throughout the experimental period (B). An intravenous glucose tolerance test (2g D-glucose with 50% [6,6-²H₂]glucose / kg body weight) was performed in 6h-fasted mice at week 11. Blood glucose levels were measured at the indicated time points (C) and the area under the curve (AUC) of the glucose excursion curve was calculated as a measure for glucose tolerance (D). Blood was also collected for determination of the time-dependent change in [6,6-²H₂]glucose concentration by gas chromatography mass spectrometry (E). For each mouse, a decay curve was fitted of which the slope represents peripheral glucose uptake (F). An i.p. insulin tolerance test (1U/kg lean body mass) was performed in 4h-fasted mice at week 11. Blood glucose levels were measured at the indicated time points (G) and the AUC of the glucose excursion curve was calculated as a measure for insulin resistance (H). After 12 weeks of infection, 4h-fasted mice received an intravenous injection of insulin (1 U/kg lean body mass) and were sacrificed by cervical dislocation after 15 minutes. Gonadal and visceral adipose tissues were collected and immediately snap-frozen. The protein expression of IRβ (I) and the phosphorylation state of PKB-Thr308 (J) were assessed by Western blot and quantified by densitometry analysis. Tubulin expression was used as internal housekeeping protein. Representative Western blots are shown (K) Results are expressed as means ± SEM. *P<0.05 HFD vs LFD, #P<0.05 helminth- vs sham-infected group. Figures C, E and G: statistical significance of HFD sham vs LFD sham and HFD infected vs HFD sham is shown (n = 12-19 animals per group in A and B and 3-11 animals per group in C-J).

Chronic *S. mansoni* infection increases adipose tissue eosinophils and alternatively activated M2 macrophages

The immune cell composition of WAT, specifically the eosinophil content and the balance between M1 and M2 macrophages, has been shown to play a crucial role in the maintenance of adipocyte insulin sensitivity and whole-body metabolic homeostasis (6). To investigate whether chronic *S. mansoni* infection affects the immune cell composition in WAT, the stromal vascular fraction (SVF) was isolated from gonadal and visceral WAT of sham- and helminth-infected mice, and the immune cell composition was analyzed by flow cytometry (see Supplemental Fig. 1 for gating strategy). We found that HFD significantly reduced B cell, NK cell, and NKT cell numbers per gram of gonadal WAT (Supplemental Fig. 2A). *S. mansoni* promoted infiltration of leukocytes into gonadal WAT, resulting in increased numbers of all lymphocyte subsets studied in both LFD- and HFD-fed mice (Supplemental Fig. 2A). No major effect of diet or infection was observed on lymphocytes in visceral WAT (Supplemental Fig. 2B).

Subsequent analysis of eosinophils, identified by CD45 and Siglec-F expression, revealed a trend for a decrease in WAT eosinophil numbers in HFD-fed mice (Fig. 3A,B), in line with a previous report (18). Chronic *S. mansoni* infection induced a strong increase in eosinophil infiltration into gonadal and visceral WATs from both LFD- and HFD-fed mice (Fig. 3A,B).

Finally, the expression of CD11c and Ym1 in CD11b⁺F4/80⁺ cells allowed us to discriminate between M1 and M2 macrophages, respectively (17) (Fig. 3C). HFD promoted a significant increase in M1 macrophages in gonadal WAT (Fig. 3D) and a decrease in M2 macrophages in visceral WAT (Fig. 3E). Analysis of adipose tissue gene expression confirmed that M1 markers were increased in HFD-fed mice, an effect particularly clear in gonadal WAT, although M2-associated genes were not down-regulated significantly (Fig. 3G,H). Chronic *S. mansoni* infection had a marginal effect on WAT M1 macrophage counts as determined by flow cytometry analysis, but strongly increased M2 macrophage numbers in both gonadal and visceral WAT from LFD- and HFD-fed mice (Fig. 3D,E), shifting the M2/M1 ratio toward M2 (Fig. 3F). In line with these results, infection induced a strong up-regulation of M2-associated genes in both gonadal and visceral WAT from LFD- and HFD-fed mice, whereas the expression of M1-related genes was barely affected (Fig. 3G,H). Lastly, mRNA expression of the type 2-associated cytokines IL-4 and IL-5 were also significantly up-regulated in WAT from helminth-infected mice (Fig. 3G,H). Taken together, these results suggest that chronic *S. mansoni* infection promotes WAT type 2 inflammation characterized by adipose tissue eosinophilia and accumulation of M2 macrophages.

***S. mansoni* soluble egg antigens improve whole-body metabolic homeostasis and promote a type 2 immune response in WAT and liver from obese mice**

To exclude that the beneficial effects of helminth infection on metabolic homeostasis are simply a result of parasitism, we next investigated whether *S. mansoni*-derived molecules can alleviate diet-induced metabolic disorders. For this purpose, HFD-fed mice were subjected to repetitive i.p. injections with SEA, which was shown to promote a strong Th2 response *in vitro* (37) and *in vivo* (38). Importantly, treatment with SEA for 4 weeks did neither affect body

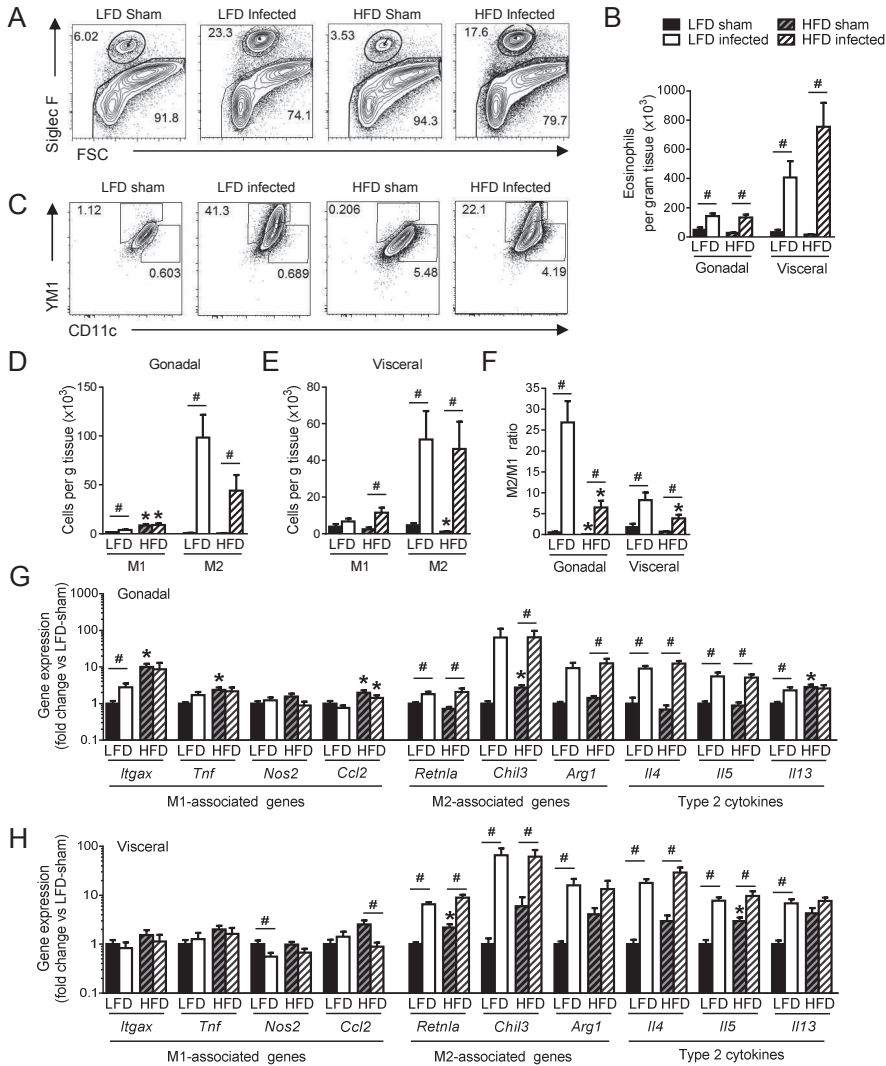


Figure 3. Chronic *S. mansoni* infection increases adipose tissue eosinophils and alternatively-activated M2 macrophages. Mice were fed a LFD or HFD and infected with *S. mansoni* as described in the legend of Fig. 1. At sacrifice (week 12), various adipose tissues were collected. Small tissue pieces were snap-frozen for qPCR analysis and the remaining tissue pieces were used for SVF isolation. Following fixation and permeabilization, SVF cells were stained and analyzed by flow cytometry. The complete gating scheme is shown in Supplemental Fig. 1. Representative flow cytometry plots from gonadal adipose tissue show the percentage of eosinophils based on Siglec-F expression in Aqua⁺CD45⁺ cells (A). The numbers of eosinophils per gram tissue were determined (B). Macrophages were identified as Aqua⁺CD45⁺Siglec-F⁺CD11b⁺F4/80⁺ cells. Representative flow cytometry plots from gonadal adipose tissue show the percentage of CD11c⁺ (M1) and Ym1⁺ (M2) macrophages (C). The numbers of M1 and M2 macrophages per gram tissue in gonadal (D) and visceral (E) WAT were determined and the M2/M1 ratios were calculated (F). mRNA expression of the indicated genes in gonadal (G) and visceral (H) adipose tissues were quantified by RT-PCR relative to RplP0 gene and expressed as fold difference compared with the non-infected LFD-fed mice. *Itgax* encodes CD11c; *Retnla* encodes Fizz1; *Chil3* encodes Ym1. Results are expressed as means \pm SEM. *P<0.05 HFD vs LFD, #P<0.05 helminth- vs sham-infected group (n = 8-16 animals per group).

weight nor lean or fat body mass (Fig. 4A), but improved fasting plasma glucose and insulin levels (Fig. 4B,C), HOMA-IR (Fig. 4C), and whole-body glucose tolerance (Fig. 4E) and insulin sensitivity (Fig. 4F).

Like the chronic parasite infection, SEA exposure promoted WAT eosinophilia (Fig. 5A), associated with accumulation of M2 macrophages (Fig. 5B), leading to a shift in the M2/M1 ratio toward M2 polarization (Fig. 5C). As we showed that helminth infection promoted gene expression of type 2-associated cytokines in WAT (Fig. 3), we next determined the numbers of CD4⁺ T cells and ILCs (lineage-negative Thy1.2⁺) in gonadal WAT (see Supplemental Fig. 1 for gating strategy), and analyzed cytokine expression by these lymphocyte subsets following stimulation with PMA and ionomycin (gating strategy shown in fig. 5E). Compared to LFD, HFD decreased the total number of CD4⁺ T cells and ILCs (Fig. 5D), and the percentage of CD4⁺ T cells expressing IL-4, but not IL-5 or IL-13 (Fig. 5F), and did not significantly affect cytokine production by ILCs (Fig. 5G). Treatment of HFD-fed mice with SEA strongly enhanced the percentage of IL-4-, IL-5- and IL-13-expressing CD4⁺ T cells in gonadal WAT (Fig. 5F), and slightly increased IL-5 production by ILCs (Fig. 5G). These findings were confirmed by quantitative PCR (qPCR), which showed that SEA promotes gene expression of M2-associated markers and type 2 cytokines (Fig. 5H).

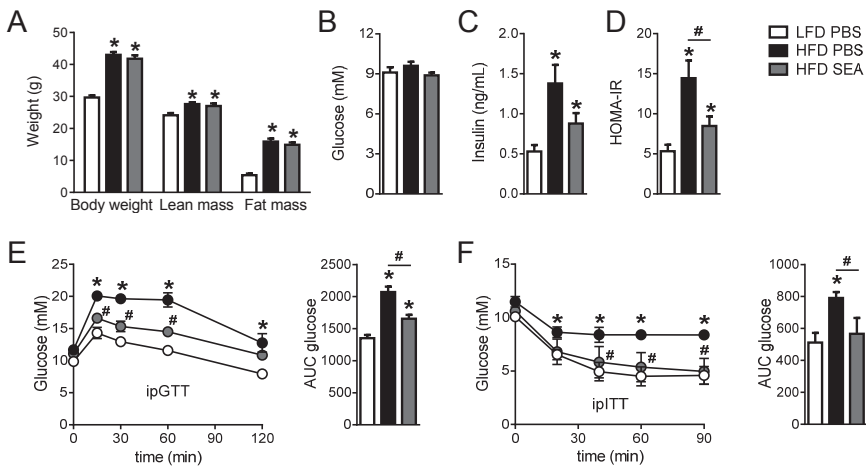


Figure 4. SEA improves whole-body metabolic homeostasis in HFD-induced obese animals. Mice were fed a LFD or HFD for 12 weeks, after which they were treated i.p. with PBS or 50 μ g SEA once every 3 days for a period of 4 weeks. Body weight and body composition were analyzed after 4 weeks of treatment (A). Plasma glucose (B) and insulin (C) levels were determined in 4h-fasted mice after 4 weeks of treatment and HOMA-IR was calculated (D). An i.p. glucose tolerance test (2 g/kg body weight) was performed in 6h-fasted mice at week 3. Blood glucose levels were measured at the indicated time points and the area under the curve (AUC) of the glucose excursion curve was calculated as a measure for glucose tolerance (E). An i.p. insulin tolerance test (1U/kg lean body mass) was performed in 4h-fasted mice at week 3. Blood glucose levels were measured at the indicated time-points, and the AUC of the glucose excursion curve was calculated as a measure for insulin resistance (F). Results are expressed as means \pm SEM. * $P < 0.05$ HFD vs LFD, # $P < 0.05$ PBS vs SEA (n = 11-13 animals per group in A-E and 3-6 animals per group in F).

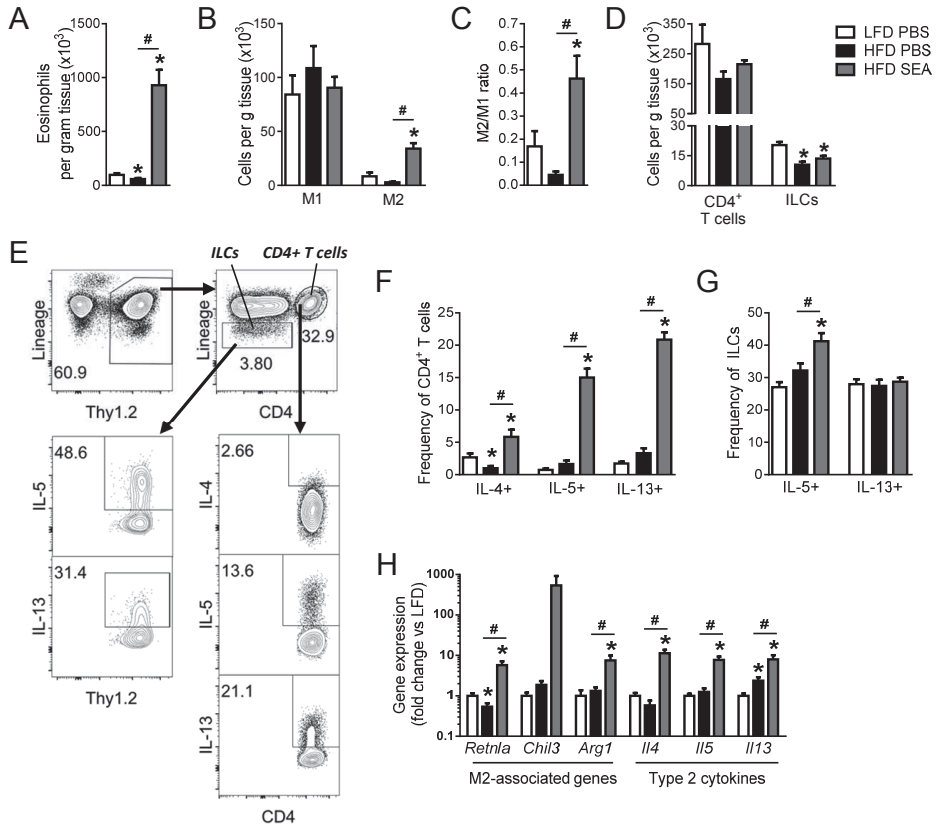


Figure 5. SEA treatment promotes adipose tissue Th2 polarization, and accumulation of eosinophils and alternatively-activated M2 macrophages. Mice were fed a LFD or HFD for 12 weeks, after which they were treated i.p. with PBS or 50 μ g SEA once every 3 days for a period of 4 weeks. At sacrifice (week 4), gonadal adipose tissue was collected and processed as described in the legend of Fig. 3. Following fixation, SVF cells were stained and analyzed by flow cytometry. Gating schemes for *ex vivo* analysis of lymphocyte subsets are shown in Supplemental Fig. 1. The numbers of eosinophils (A) and M1 and M2 macrophages (B) per gram tissue were determined, and the M2/M1 ratio was calculated (C). The numbers of CD4⁺ T cells and ILCs were determined (D). Intracellular cytokine production was analyzed after 4h stimulation with PMA and ionomycin in the presence of brefeldin A. Following gating on Aqua⁺CD45⁺ cells, lymphocyte subsets were analyzed by selecting for Thy1.2⁺ cells to enrich for T cells and ILCs. CD4⁺ T cells were subsequently identified as Lineage⁺CD4⁺ cells, in which the lineage cocktail included antibodies against CD3, CD11b, CD11c, B220, GR-1 and NK1.1. ILCs were identified as Lineage⁺CD4⁺ cells. Representative flow cytometry plots show the gating strategy for analysis of cytokine-expressing CD4⁺ T cells and ILCs (E). The frequencies of cytokine-expressing T cells (F) and ILCs (G) were determined. mRNA expression of the indicated genes was analyzed as described in the legend of Fig. 3 (H). *Retnla* encodes Fizz1; *Chil3* encodes Ym1. Results are expressed as means \pm SEM. * $P < 0.05$ HFD vs LFD, # $P < 0.05$ PBS vs SEA (n = 9-13 animals per group for all measurements except for intracellular analysis of IL-5 (n = 3-7)).

As classical activation of liver macrophages has also been observed in diet-induced obesity (39), we determined the effect of SEA treatment on the hepatic immune cell composition. Analysis of myeloid cells showed that HFD did not affect liver eosinophil numbers (Fig. 6A). Assessment of CD45⁺Siglec-F⁺CD11b^{lo}F4/80^{hi} macrophages (Fig. 6B), which were identified previously as Kupffer cells (40), showed that HFD promoted CD11c expression in these cells with no effect on Ym1 expression (Fig. 6C), thereby strongly decreasing the Ym1/CD11c ratio (Fig. 6D). HFD also decreased the numbers of CD4⁺T cells and ILCs (Fig. 6E), although analysis of cytokine production (Fig. 6F) showed that HFD did not affect expression of Th2 cytokines by T cells (Fig. 6G). HFD reduced the frequency of IL-5- and IL-13-expressing ILCs (Fig. 6G). SEA injections promoted eosinophil infiltration (Fig. 6A), but did not affect macrophage polarization (Fig. 6B,C), which was also confirmed by qPCR analysis (Fig. 6I). In line with our findings in WAT, SEA strongly increased expression of IL-4, IL-5 and IL-13 by CD4⁺ T cells in the liver (Fig. 6G), without a pronounced effect on the expression of type 2 cytokines by ILCs (Fig. 6H). Taken together, these findings indicate that helminth-derived molecules improve metabolic homeostasis, associated with the induction of eosinophils and Th2 cells in WAT and liver, and M2 macrophage polarization in WAT.

DISCUSSION

Over the past decade, it has become increasingly clear that multiple facets of the Th2-associated immune response promote metabolic homeostasis (6). Landmark studies have shown that infection of diet-induced obese mice with the rodent nematode *N. brasiliensis* ameliorates whole-body insulin sensitivity and glucose tolerance (18;26). In the present study, we analyzed which aspects of whole-body energy metabolism and WAT immune cell composition are affected by helminths, using a model of chronic *S. mansoni* infection. Unlike *N. brasiliensis*, which gives a strong Th2 response that mediates parasite clearance within two weeks, *S. mansoni* establishes a chronic infection, characterized by the presence of Th2 cells, alternatively activated macrophages, and a regulatory network (29). To study the effect of Th2-inducing conditions in a pathogen-free setting, we next exposed mice on a HFD to repetitive injections with *S. mansoni* soluble egg antigens.

We report that chronic exposure to *S. mansoni* induces a type 2 immune response in adipose tissue and improves both insulin sensitivity and glucose tolerance. These findings indicate that the beneficial effect of chronic *S. mansoni* infection on whole-body metabolic homeostasis, as reported previously for short-lived infection with *N. brasiliensis* (18;26), is a hallmark of helminth infection. Unique to our study, we have performed in-depth metabolic profiling, which showed that helminth infection specifically reduced fat mass and dampened HFD-induced adipocyte hypertrophy. However, we surprisingly did not find any changes in food intake or energy expenditure in our experimental conditions, leading us to speculate that chronic *S. mansoni* infection may affect nutrient efficiency by impairing intestinal lipid absorption. Another possibility is that dietary fat could be incorporated into eggs by the worms and next excreted through the feces. Further studies are required to clarify this specific

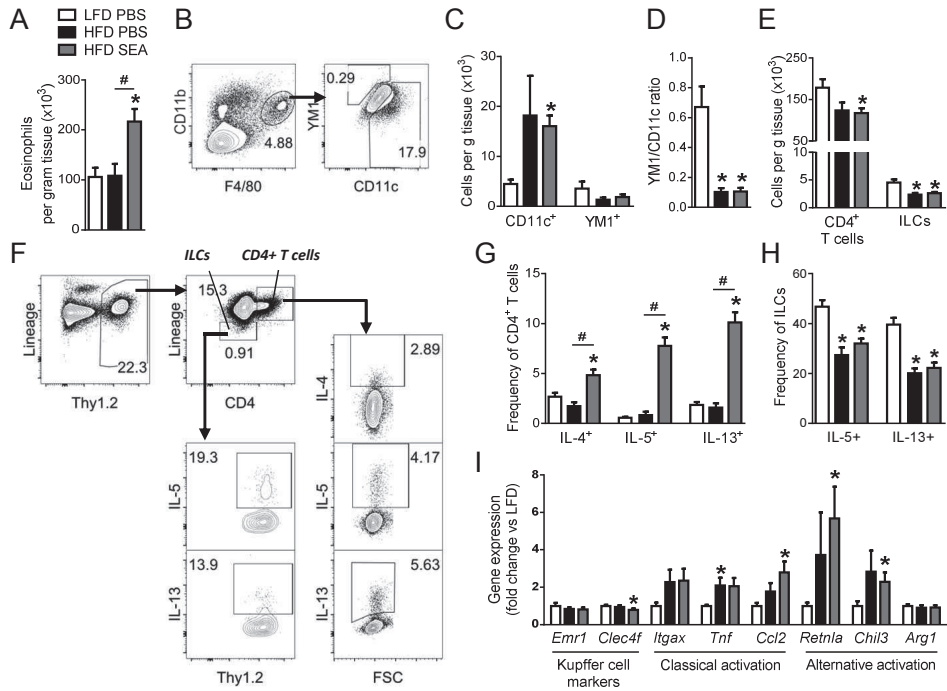


Figure 6. SEA treatment promotes accumulation of eosinophils and Th2 polarization in liver. Mice were fed a LFD or HFD for 12 weeks, after which they were treated i.p. with PBS or 50 μ g SEA once every 3 days for a period of 4 weeks. At sacrifice, livers were collected and a small piece was snap-frozen for qPCR analysis. From the remaining liver tissue, CD45⁺ cells were isolated and analyzed by flow cytometry. Gating schemes for *ex vivo* analysis of lymphocyte subsets are shown in Supplemental Fig. 1. The numbers of eosinophils (A) were determined. Kupffer cells were gated based on CD11b and F4/80 expression in Aqua CD45⁺Siglec-F⁺ cells (B). The number of CD11c⁺ and Ym1⁺ Kupffer cells (C) per gram liver were determined, and the Ym1⁺/CD11c⁺ ratio was calculated (D). The numbers of CD4⁺T cells and ILCs were determined (E). Intracellular cytokine expression was analyzed as described in the legend of Fig. 5. The gating strategy for analysis of cytokine-expressing CD4⁺T cells and ILCs is shown (F). The frequencies of cytokine-expressing CD4⁺T cells (G) and ILCs (H) were determined. mRNA expression of the indicated genes was analyzed as described in the legend of Fig. 3 (I). *Emr1* encodes F4/80; *Itgax* encodes CD11c; *Retnla* encodes Fizz1; *Chil3* encodes Ym1. Results are expressed as means \pm SEM. * $P < 0.05$ HFD vs LFD, # $P < 0.05$ WT vs Mrc1 (n = 11-13 animals per group).

point. Remarkably, infection improved fasting plasma glucose and insulin levels, whole-body glucose tolerance and insulin sensitivity in HFD-fed mice. Among the possible underlying mechanisms, we found that *S. mansoni* reversed HFD-induced inhibition of peripheral glucose uptake, which may be secondary to tissue-specific improvement of insulin sensitivity, as *S. mansoni*-infected HFD-fed mice exhibited higher insulin-induced PKB phosphorylation in WAT than uninfected controls.

Except for small effects on adipocyte volume, fasting insulin and energy expenditure, none of the metabolic parameters analyzed were affected by *S. mansoni* infection in mice on LFD, suggesting that helminths improve metabolic homeostasis independently of putative

S. mansoni-induced pathologies. We cannot exclude the possibility that part of the effect may be secondary to body weight loss or increased glucose/lipid metabolism by the helminths themselves. However, sustained exposure to SEA did not significantly affect body weight, but improved HOMA-IR, whole-body glucose tolerance and insulin sensitivity, in line with a previous report (41). Taken together, these findings suggest that the beneficial effects of helminths on metabolic homeostasis are not secondary to parasitism on host metabolism, but likely due to a direct effect on metabolic tissues or immune cells.

We demonstrate that *S. mansoni* infection reduced diet-induced body weight gain and improved HOMA-IR, once infection was established beyond 6 weeks. Glucose tolerance and peripheral glucose uptake were also improved after 11 but not 5 weeks of infection (Supplemental Fig. 3). Since egg production by adult worms triggers the development of a type 2 response ~6 weeks after infection (42), it is therefore likely that the beneficial effect of helminths on metabolic homeostasis may be mediated by the presence of eggs. This is further supported by our data showing that *S. mansoni* egg-derived soluble molecules improve glucose tolerance and insulin sensitivity in HFD-fed mice. Interestingly, improvements in metabolic homeostasis were also found in obese mice treated with the Lewis^x-containing glycan LNFPIII (41). Of note, we have demonstrated previously that omega-1, a Lewis^x-containing immunomodulatory RNase isolated from SEA, skews strong Th2 responses (43;44). Whether omega-1 contributes to the beneficial effect of helminth infection or SEA injection on energy homeostasis requires further study.

It is well-established that adipocyte hypertrophy in response to HFD induces cell necrosis, leading to the infiltration of M1 macrophages which later form crown-like structures around the necrotic cells (45;46). Chronic *S. mansoni* infection did not reduce M1 gene expression or cell numbers, suggesting that M1 macrophages continue to reside in WAT, even though glucose homeostasis improves. In line with this, SEA injections did not affect M1 cell numbers. These findings differ from a study by Fujisaka *et al.* (47) in which the anti-diabetic drug pioglitazone reduced expression of the CD11c-encoding gene, and lowered M1 cell numbers in gonadal WAT in HFD-fed mice. In addition, both infection with *N. brasiliensis* and pioglitazone treatment reduced total WAT macrophages (18;47), whereas chronic *S. mansoni* infection or SEA administration increased WAT macrophage numbers, as a result of an increase in M2 numbers. Taken together, these findings indicate that the M2/M1 ratio, rather than an increase or decrease in a particular macrophage subset, might be critical for metabolic homeostasis.

Mechanistically, the rise in WAT M2 macrophage numbers following chronic *S. mansoni* infection or repeated SEA administration may be a result of local macrophage proliferation, which has been reported in the pleural cavity upon infection with the filarial helminth *Litomosoides sigmodontis* in response to IL-4 (48). An alternative explanation could be that *S. mansoni* or SEA induce WAT monocyte infiltration and differentiation into M2 macrophages, which is plausible since we observed a significant increase in blood CD11b⁺Ly6C⁺ inflammatory Ym1-expressing monocytes during chronic infection (data not shown). Of note, it is rather unlikely that helminth-derived molecules trigger M2 polarization by directly interacting with

macrophages, as it has been described that SEA treatment does not induce expression of *Chil3* (encoding *Ym1*), *Mrc1* and *Arg1* by bone marrow-derived macrophages *in vitro* (27).

Importantly, it was demonstrated recently that maintenance of M2 macrophages in WAT depends on the presence of IL-4-secreting eosinophils (18), which are sustained by IL-5- and IL-13-producing ILC2s (19). In our study, we showed that chronic *S. mansoni* infection and SEA treatment promoted eosinophil accumulation in WAT, consistent with a previous reports on *N. brasiliensis* infection (18;19), and increased the mRNA levels of the type 2 cytokines IL-4 and IL-5. By analyzing intracellular IL-4, IL-5 and IL-13 cytokine production by lymphocytes isolated from gonadal WAT of SEA-treated mice, we found that CD4⁺ T cells, but not ILCs, produced increased levels of these type 2 cytokines. Recent literature described that IL-13 production by ILC2s in response to *S. mansoni* egg challenge peaks after 7 days of challenge and is reduced to baseline by day 21 (49). Since we analyze cytokine responses after 4 weeks of SEA administration, we speculate that ILC2 cytokine production has already diminished. Therefore, it is still possible that *S. mansoni*-induced ILC2s may be the first trigger for eosinophilia and accumulation of M2 macrophages in WAT. Then, at a later stage of infection or after long-term helminth antigen exposure, Th2-derived cytokines such as IL-4 may mediate M2 proliferation (48). Of note, we analyzed expression of a variety of eosinophil-attracting chemokines and eotaxins in WAT, but found no effect of SEA treatment (data not shown). Taken together, the interaction between the different cell types involved, as well as their relative contribution to the beneficial effect of helminths on WAT insulin sensitivity and whole-body metabolic homeostasis, requires further studies.

In addition to profound effects of SEA treatment on immune cells in WAT, we also observed increased eosinophilia and Th2 cytokine expression in the liver, suggesting that the adipose tissue is not an exclusive target of *S. mansoni*-derived antigens. Interestingly, it has been reported that both IL-4 and IL-13 may contribute to glucose homeostasis by directly regulating hepatic insulin sensitivity and glucose production, respectively (21;50). Helminth molecules may indeed work as a double-edged sword, acting on inflammatory and metabolic pathways in WAT and liver. The exact contribution of the liver to the whole-body metabolic beneficial phenotype observed in response to SEA treatment remains to be clarified.

In conclusion, our work has revealed that chronic infection with *S. mansoni*, as well as SEA treatment, protects against metabolic disorders in a mouse model of HFD-induced obesity. We have established that *S. mansoni* reduces adipocyte size and promotes peripheral glucose uptake and WAT-specific insulin sensitivity. Through analysis of immune cell composition at the cellular level, we show that SEA injections strongly increase eosinophils and Th2 cells in both WAT and liver, although they only promote M2 macrophage polarization in WAT. Collectively, our data identify *S. mansoni*-derived egg antigens as attractive agents for therapeutic manipulation of the immune system in the context of metabolic disorders. Several clinical trials are currently registered to assess the safety or efficacy of helminth therapy for the treatment of various inflammatory diseases in humans. As helminth infections can induce pathological conditions, studies are now focusing on helminth-derived molecules (51;52). The identification of single active molecules and the mechanisms by which they improve whole-body metabolic

homeostasis may offer new insights toward the development of novel therapeutics for the treatment of metabolic syndrome.

ACKNOWLEDGEMENTS

The authors also thank Bart Everts (LUMC, Leiden, The Netherlands) for critically reading the manuscript. This work was supported by an EFSD/Lilly Research Grant Fellowship from the European Federation for the Study of Diabetes (to BG), a Scientific Programme Indonesia-Netherlands-The Royal Netherlands Academy of Sciences Grant (SPIN-KNAW; KNAW-57-SPIN3-JRP; to MY and BG), the EU-funded project IDEA (HEALTH-F3-2009-241642; to MY), a ZonMW TOP Grant from the Dutch Organization for Scientific Research (91214131; to MY and BG), and a grant from the Board of Directors of the Leiden University Medical Center (to VvH).

REFERENCES

1. Calle EE, et al. Overweight, obesity, and mortality from cancer in a prospectively studied cohort of U.S. adults. *N Engl J Med* 2003 Apr 24;348(17):1625-38.
2. Herman WH, et al. Type 2 diabetes: an epidemic requiring global attention and urgent action. *Diabetes Care* 2012 May;35(5):943-4.
3. Ouchi N, et al. Adipokines in inflammation and metabolic disease. *Nat Rev Immunol* 2011 Feb;11(2):85-97.
4. Weisberg SP, et al. Obesity is associated with macrophage accumulation in adipose tissue. *J Clin Invest* 2003 Dec;112(12):1796-808.
5. Xu H, et al. Chronic inflammation in fat plays a crucial role in the development of obesity-related insulin resistance. *J Clin Invest* 2003 Dec;112(12):1821-30.
6. Chawla A, et al. Macrophage-mediated inflammation in metabolic disease. *Nat Rev Immunol* 2011 Nov;11(11):738-49.
7. Hotamisligil GS, et al. IRS-1-mediated inhibition of insulin receptor tyrosine kinase activity in TNF- α - and obesity-induced insulin resistance. *Science* 1996 Feb 2;271(5249):665-8.
8. Hotamisligil GS, et al. Adipose expression of tumor necrosis factor- α : direct role in obesity-linked insulin resistance. *Science* 1993 Jan 1;259(5091):87-91.
9. Feingold KR, et al. Stimulation of lipolysis in cultured fat cells by tumor necrosis factor, interleukin-1, and the interferons is blocked by inhibition of prostaglandin synthesis. *Endocrinology* 1992 Jan;130(1):10-6.
10. Green A, et al. Tumor necrosis factor increases the rate of lipolysis in primary cultures of adipocytes without altering levels of hormone-sensitive lipase. *Endocrinology* 1994 Jun;134(6):2581-8.
11. Rosen ED, et al. Adipocytes as regulators of energy balance and glucose homeostasis. *Nature* 2006 Dec 14;444(7121):847-53.
12. Talukdar S, et al. Neutrophils mediate insulin resistance in mice fed a high-fat diet through secreted elastase. *Nat Med* 2012 Sep;18(9):1407-12.
13. Liu J, et al. Genetic deficiency and pharmacological stabilization of mast cells reduce diet-induced obesity and diabetes in mice. *Nat Med* 2009 Aug;15(8):940-5.
14. Winer DA, et al. B cells promote insulin resistance through modulation of T cells and production of pathogenic IgG antibodies. *Nat Med* 2011 May;17(5):610-7.
15. DeFuria J, et al. B cells promote inflammation in obesity and type 2 diabetes through regulation of T-cell function and an inflammatory cytokine profile. *Proc Natl Acad Sci USA* 2013 Mar 26;110(13):5133-8.
16. Nishimura S, et al. CD8+ effector T cells contribute to macrophage recruitment and adipose tissue inflammation in obesity. *Nat Med* 2009 Aug;15(8):914-20.
17. Lumeng CN, et al. Obesity induces a phenotypic switch in adipose tissue macrophage polarization. *J Clin Invest* 2007 Jan;117(1):175-84.
18. Wu D, et al. Eosinophils sustain adipose alternatively activated macrophages associated with glucose homeostasis. *Science* 2011 Apr 8;332(6026):243-7.
19. Molofsky AB, et al. Innate lymphoid type 2 cells sustain visceral adipose tissue eosinophils and alternatively activated macrophages. *J Exp Med* 2013 Mar 11;210(3):535-49.
20. Winer S, et al. Normalization of obesity-associated insulin resistance through immunotherapy. *Nat Med* 2009 Aug;15(8):921-9.
21. Ricardo-Gonzalez RR, et al. IL-4/STAT6 immune axis regulates peripheral nutrient metabolism and insulin sensitivity. *Proc Natl Acad Sci USA* 2010 Dec 28;107(52):22617-22.
22. Feuerer M, et al. Lean, but not obese, fat is enriched for a unique population of regulatory T cells that affect metabolic parameters. *Nat Med* 2009 Aug;15(8):930-9.
23. Chen Y, et al. Association of previous schistosome infection with diabetes and metabolic syndrome: a cross-sectional study in rural China. *J Clin Endocrinol Metab* 2013 Feb;98(2):E283-E287.
24. Aravindhan V, et al. Decreased prevalence of lymphatic filariasis among diabetic subjects associated with a diminished pro-inflammatory cytokine response (CURES 83). *PLoS Negl Trop Dis* 2010;4(6):e707.
25. Wiria AE, et al. Helminth infections, type-2 immune response, and metabolic syndrome. *PLoS Pathog* 2014 Jul;10(7):e1004140.
26. Yang Z, et al. Parasitic nematode-induced modulation of body weight and associated metabolic dysfunction in mouse models of obesity. *Infect Immun* 2013 Jun;81(6):1905-14.

27. Wolfs IM, et al. Reprogramming macrophages to an anti-inflammatory phenotype by helminth antigens reduces murine atherosclerosis. *FASEB J* 2014 Jan;28(1):288-99.
28. World Health Organization. Schistosomiasis. <http://www.who.int/schistosomiasis/en/> 2013 Available from: URL: <http://www.who.int/schistosomiasis/en/>
29. Dunne DW, et al. A worm's eye view of the immune system: consequences for evolution of human autoimmune disease. *Nat Rev Immunol* 2005 May;5(5):420-6.
30. Maizels RM, et al. Immune regulation by helminth parasites: cellular and molecular mechanisms. *Nat Rev Immunol* 2003 Sep;3(9):733-44.
31. Hussaarts L, et al. Regulatory B-cell induction by helminths: implications for allergic disease. *J Allergy Clin Immunol* 2011 Oct;128(4):733-9.
32. Smits HH, et al. Protective effect of *Schistosoma mansoni* infection on allergic airway inflammation depends on the intensity and chronicity of infection. *J Allergy Clin Immunol* 2007 Oct;120(4):932-40.
33. Ackermans MT, et al. The quantification of gluconeogenesis in healthy men by (2)H₂O and [2-(13)C]glycerol yields different results: rates of gluconeogenesis in healthy men measured with (2)H₂O are higher than those measured with [2-(13)C]glycerol. *J Clin Endocrinol Metab* 2001 May;86(5):2220-6.
34. van den Berg SA, et al. High levels of dietary stearate promote adiposity and deteriorate hepatic insulin sensitivity. *Nutr Metab (Lond)* 2010;7:24.
35. Jo J, et al. Hypertrophy and/or Hyperplasia: Dynamics of Adipose Tissue Growth. *PLoS Comput Biol* 2009 Mar;5(3):e1000324.
36. Geerling JJ, et al. Metformin Lowers Plasma Triglycerides by Promoting VLDL-Triglyceride Clearance by Brown Adipose Tissue in Mice. *Diabetes* 2014 Mar;63(3):880-91.
37. de Jong EC, et al. Microbial compounds selectively induce Th1 cell-promoting or Th2 cell-promoting dendritic cells in vitro with diverse th cell-polarizing signals. *J Immunol* 2002 Feb 15;168(4):1704-9.
38. Okano M, et al. Induction of Th2 responses and IgE is largely due to carbohydrates functioning as adjuvants on *Schistosoma mansoni* egg antigens. *J Immunol* 1999 Dec 15;163(12):6712-7.
39. Morinaga H, et al. Characterization of Distinct Subpopulations of Hepatic Macrophages in HFD/Obese Mice. *Diabetes* 2014 Oct 14;
40. Movita D, et al. Kupffer cells express a unique combination of phenotypic and functional characteristics compared with splenic and peritoneal macrophages. *J Leukoc Biol* 2012 Oct;92(4):723-33.
41. Bhargava P, et al. Immunomodulatory glycan LNFP III alleviates hepatosteatosis and insulin resistance through direct and indirect control of metabolic pathways. *Nat Med* 2012 Nov;18(11):1665-72.
42. Pearce EJ, et al. The immunobiology of schistosomiasis. *Nat Rev Immunol* 2002 Jul;2(7):499-511.
43. Everts B, et al. Omega-1, a glycoprotein secreted by *Schistosoma mansoni* eggs, drives Th2 responses. *J Exp Med* 2009 Aug 3;206(8):1673-80.
44. Everts B, et al. Schistosome-derived omega-1 drives Th2 polarization by suppressing protein synthesis following internalization by the mannose receptor. *J Exp Med* 2012 Sep 24;209(10):1753-67, S1.
45. Pajvani UB, et al. Fat apoptosis through targeted activation of caspase 8: a new mouse model of inducible and reversible lipodystrophy. *Nat Med* 2005 Jul;11(7):797-803.
46. Cinti S, et al. Adipocyte death defines macrophage localization and function in adipose tissue of obese mice and humans. *J Lipid Res* 2005 Nov;46(11):2347-55.
47. Fujisaka S, et al. Regulatory mechanisms for adipose tissue M1 and M2 macrophages in diet-induced obese mice. *Diabetes* 2009 Nov;58(11):2574-82.
48. Jenkins SJ, et al. Local macrophage proliferation, rather than recruitment from the blood, is a signature of TH2 inflammation. *Science* 2011 Jun 10;332(6035):1284-8.
49. Hams E, et al. IL-25 and type 2 innate lymphoid cells induce pulmonary fibrosis. *Proc Natl Acad Sci USA* 2014 Jan 7;111(1):367-72.
50. Stanya KJ, et al. Direct control of hepatic glucose production by interleukin-13 in mice. *J Clin Invest* 2013 Jan 2;123(1):261-71.
51. Harnett W, et al. Helminth-derived immunomodulators: can understanding the worm produce the pill? *Nat Rev Immunol* 2010 Apr;10(4):278-84.
52. Wammes LJ, et al. Helminth therapy or elimination: epidemiological, immunological, and clinical considerations. *Lancet Infect Dis* 2014 Nov;14(11):1150-62.

SUPPLEMENTAL DATA

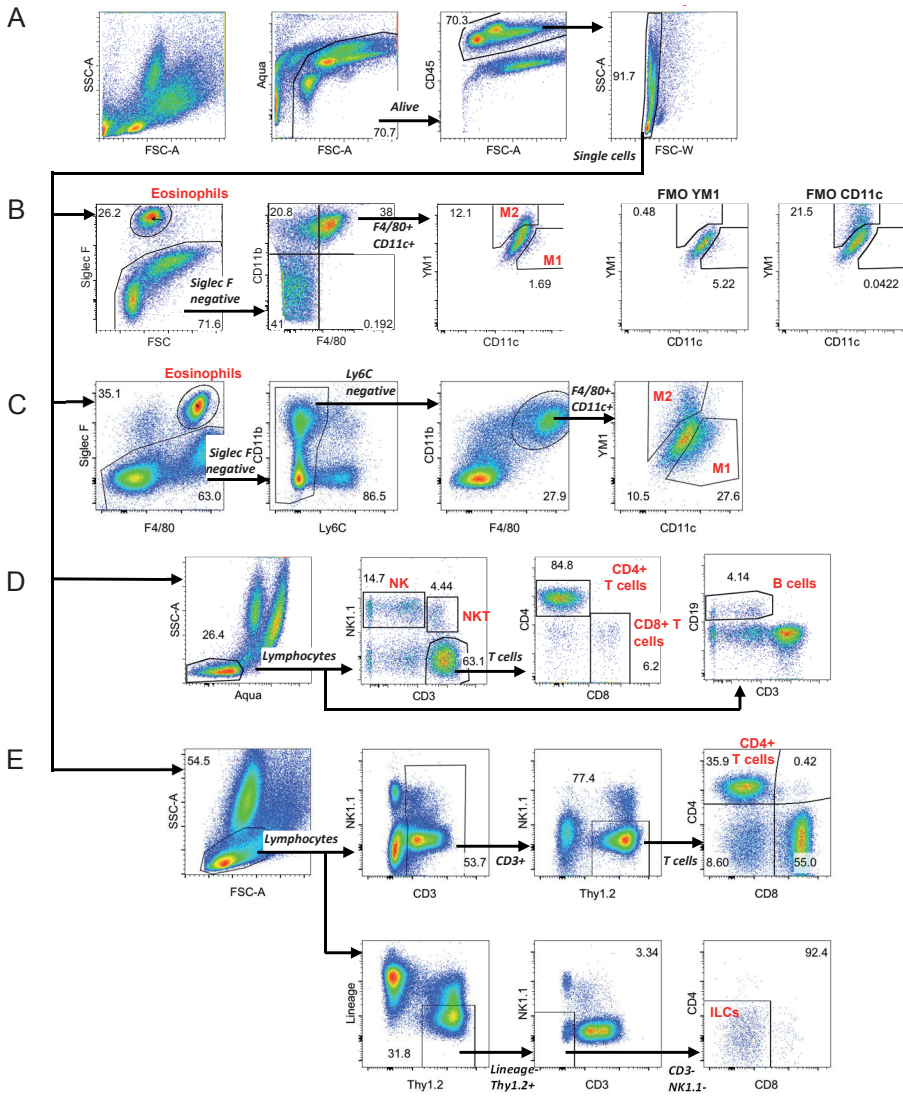


Figure S1. Gating strategies. Isolated cells were pre-gated on Aqua CD45⁺ single cells (A). The gating strategy for analysis of eosinophils, CD11c⁻ M1 macrophages and Ym1⁺ M2 macrophages is shown, including Fluorescence Minus One (FMO) controls for Ym1 and CD11c, in a representative sample from the chronic infection study (B) and the i.p. injection study (C). The gating strategy is shown for NK cells, NKT cells, CD4⁺ T cells, CD8⁺ T cells and B cells in a representative sample from the chronic infection study (D), and for CD4⁺ T cells and innate lymphoid cells (ILCs) in a representative sample from the i.p. study (E). For *ex vivo* analysis of CD4⁺ T cells and ILCs, the lineage cocktail included antibodies against CD11b, CD11c, B220 and GR-1. Note: Gating on CD4⁺ T and ILCs with CD3 in the lineage channel gave similar results. Representative samples were chosen from gonadal adipose tissue; gating strategies were similar for the analysis of myeloid and lymphoid subsets in visceral adipose tissue and liver.

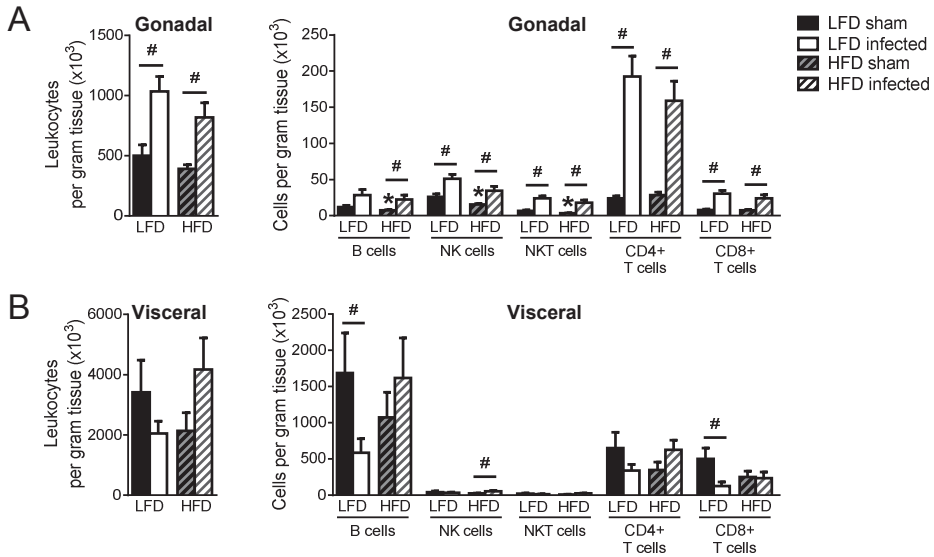


Figure S2. Lymphocyte composition of WAT. Mice were fed a LFD or a HFD for 6 weeks before infection with *S. mansoni* cercariae or sham-infection for 12 weeks. At sacrifice (week 12), various adipose tissues were collected and their stromal vascular fractions (SVF) were isolated. Following fixation, SVF cells were stained and analyzed by flow cytometry. The gating strategy is shown in figure S1D. The numbers of CD45⁺ leukocytes and indicated lymphocyte populations per gram tissue for gonadal (A) and visceral (B) WAT were determined. Results are expressed as means \pm SEM. * $P < 0.05$ vs LFD, # $P < 0.05$ vs sham-infected group (n = 12-18 animals per group in A, and 5-13 animals per group in B).

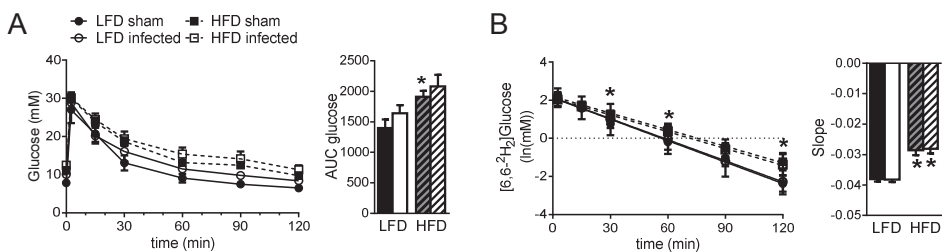


Figure S3. *S. mansoni* infection does not affect glucose tolerance or uptake after 5 weeks of infection. Mice were fed a LFD or a HFD and were infected with *S. mansoni* as described in the legend of Fig. S2. An intravenous glucose tolerance test (2g D-glucose with 50% [6,6-²H₂]glucose / kg BW) was performed in 6h-fasted mice at week 5. Blood glucose levels were measured at the indicated time points and the area under the curve (AUC) of the glucose excursion curve was calculated (A). Blood was also collected for determination of the time-dependent change in [6,6-²H₂]glucose concentration by gas chromatography mass spectrometry. For each mouse, a decay curve was fitted of which the slope represents peripheral glucose uptake (B). Results are expressed as means \pm SEM. * $P < 0.05$ vs LFD (n = 4-11 animals per group).

